

# Coarsening Kinetics of Pb Phase in a Nanocomposite Alloy Produced by Mechanical Alloying in Immiscible Al-Pb System and the Influence of Cu Addition on It

Wu Zhifang, Liu Chao, Wu Run, Chang Qingming

*The State Key Laboratory of Refractories and Metallurgy, Wuhan University of Science and Technology, Wuhan 430081, China*

**Abstract:** Coarsening kinetics of Pb phase in a nanocomposite alloy produced by mechanical alloying in immiscible Al-Pb system and the influence of Cu addition on it were studied by X-ray diffraction, scanning electron microscopy and transmission electron microscopy. Results show that when annealing at 573, 623, 673 and 723 K for different time, the relation of average particle size of Pb phase in Al-Pb nanocomposite alloys to time obeys the cube law even though the size of the constituent phase is in the nanometer range. The coarsening activation energy of Pb phase is 84.8 kJ/mol, close to the grain boundary self-diffusion activation energy of Al matrix. This indicates that the coarsening of Pb phase is controlled by grain boundary diffusion. Adding Cu decreases the coarsening rate of Pb phase, primarily by reducing the interfacial energy through Cu segregation at the Al/Pb interface. The coarsening activation energy of Pb phase is increased by the addition of Cu.

**Key words:** mechanical alloying; aluminum alloys; coarsening; nanocomposite alloys

Binary immiscible alloy systems, such as Al-Pb, Cu-Ag, Fe-Cu, Cu-W and Cu-Co, are characterized by positive heat of mixing ( $\Delta H > 0$ ), and the miscibility of components in such systems is very low or even virtually absent in both solid and liquid states except at very high temperatures<sup>[1]</sup>. It had been revealed that different metastable phases, such as supersaturated solid solution, amorphous and nanocomposite, which usually lead to unique properties, have been synthesized in such systems with highly non-equilibrium processing methods such as mechanical alloying (MA)<sup>[2-4]</sup>. Nanocomposite alloys, which consist of at least two phases in nanometer size, have potential application in the fields of magnetic materials<sup>[5]</sup>, hydrogen storage materials<sup>[6]</sup>, hard metals<sup>[7]</sup>, bearing alloys<sup>[8]</sup>, and so on. It has also been revealed that the nanocomposite alloys prepared by MA in binary immiscible systems exhibit superior properties, such as giant magnetoresistance shown in the Cu-Co nanocomposite alloy<sup>[9]</sup>, and the evidently improved wear properties of the Al-Sn nanocomposite alloy<sup>[10]</sup>. However, the

nanocomposite alloys obtained by MA in binary immiscible systems are in powder form and sintering process is required to consolidate the powder into bulk form. In this case the structure stability of nanocomposite alloys is very important because their significant high fraction of grain boundary provides a strong driving force for grain growth and results in change of properties. Thus, to clarify the growth behavior of nanocomposite alloys in the sintering process is of great importance.

For the conventional grain sized composite alloys, the self-similar coarsening of dispersed spherical particles embedded in a matrix, also known as Ostwald ripening, is generally described by Lifshitz-Slyozov-Wagner (LSW) theory<sup>[11,12]</sup>. The LSW theory states that the cube of the average particle radius grows proportional with the annealing time if the mass transport is governed by a diffusion mechanism. Since interparticle diffusional interactions are neglected in LSW theory, this theory is strictly valid only in the physically unrealistic limit of zero

Received date: December 25, 2016

Foundation item: National Natural Science Foundation of China (51201118); Foundation of the State Key Laboratory of Refractories and Metallurgy (2016QN11); KLGHEI (KLB11003)

Corresponding author: Wu Zhifang, Ph. D., Associate Professor, The State Key Laboratory of Refractories and Metallurgy, Wuhan University of Science and Technology, Wuhan 430081, P. R. China, Tel: 0086-27-68862234, E-mail: wuzhifang@wust.edu.cn

Copyright © 2017, Northwest Institute for Nonferrous Metal Research. Published by Elsevier BV. All rights reserved.

volume fraction of secondary phase. Many efforts have been made to modify LSW theory and extend it to nonzero volume fraction of dispersed phases using both analytic and numerical methods. All these modern Ostwald ripening theories show that the cubic growth law can still be used for embedded phase of high volume fraction, with the coarsening rate being dependent on the volume fraction<sup>[13,14]</sup>. In addition, many experiments were performed involving the effect of particle shape<sup>[15]</sup> and elastic stress<sup>[16]</sup>, as well as alloying addition<sup>[17]</sup>. The result shows that the shape of secondary phase has no distinct effect on coarsening kinetics<sup>[15]</sup>. It has also been found that alloying addition and elastic stress have apparent effects on coarsening behavior of secondary phase. For instance, additions of Cr and Ni reduce the coarsening rate of the precipitate in Al-Cu-Mg alloys, while additions of Li and Si significantly increase the coarsening rate<sup>[17]</sup>. Further investigation is necessary to have thorough understanding on the influence of adding elements.

Binary immiscible alloy systems are ideal systems for investigating the coarsening kinetics of secondary phase due to the fact the two phases being constant in the coarsening process. For the nanocomposite alloys produced by MA in such systems, the results show that the coarsening of secondary phase still follows the LSW theory and the coarsening activation energy of secondary phase is different from that of conventional grain sized alloys<sup>[18,19]</sup>. Actually, the LSW theory assumes zero volume fraction of secondary phase, which is obviously not suitable for the case of nanocomposite alloys due to their high volume fractions of secondary phases (26.6%~50.88%). For the nanocomposite alloys, the interparticle diffusion interactions are more remarkable owing to their unique structure. Therefore, it's necessary to take into account the effect of volume fraction to investigate the coarsening kinetics and the coarsening activation energy of secondary phase with nonzero volume fraction in the nanocomposite alloys. In addition, the influence of alloying addition on coarsening kinetics of secondary phase in the nanocomposite alloys has seldom been studied.

In the present work, the coarsening kinetics of Pb phase with very small volume fraction in the sintering process of ball milled Al-Pb and the effect of Cu addition were studied. This is because Al-Pb is a typical immiscible system and the Al-Pb nanocomposite alloys fabricated by MA exhibit super wear resistance which is very much dependent on the grain size (and/or phase size)<sup>[8]</sup> and the addition of a small amount of the third constituent such as Cu<sup>[20]</sup>. Therefore, a study of coarsening kinetics of Pb phase with very small volume fraction in Al-Pb nanocomposite alloys and the influence of Cu addition is significant to both the fundamental research of nanocomposite alloys and their application in engineering.

## 1 Experiment

Al, Pb and Cu powders of 99.9% purity with the average particle size of 70~80  $\mu\text{m}$  were used as raw materials. One alloy with composition of Al-5wt%Pb was selected, in which the volume fraction of Al and Pb phase is 99.32% and 0.68%, respectively, and Al and Pb are hence regarded as matrix phase and secondary phase with very small volume fraction, respectively. Another alloy with composition of Al-5wt%Pb-4.5wt%Cu was selected to investigate the effect of addition of Cu on coarsening kinetics of Pb phase. The powder mixtures of selected compositions were sealed in stainless steel vials together with hardened steel balls. The weight ratio of the powder to ball was 1 to 10. The handling of powders was performed inside a glove box filled with pure argon. The milling process was performed in a QM-3SP2 planetary ball mill. The milled powders were uni-axially cold pressed under a pressure of 440 MPa to get bulk samples. The as-compacted bulk samples were then sintered at different temperatures for different time under the protection of pure argon atmosphere. Then the samples were characterized by X-ray diffraction (Philips X'Pert MPD with Cu-K $\alpha$  radiation), scanning electron microscopy (SEM, FEI-Navo Nano SEM 400) and transmission electron microscopy (TEM, JEM-2100). Element mapping was performed in a VG HB601 STEM to reveal the composition of the phases. Thin foils for TEM observation were prepared by ion milling.

## 2 Results and Discussion

### 2.1 Coarsening kinetics of Pb phase in Al-5wt%Pb nanocomposite alloys produced by ball milling

Fig.1 shows the X-ray diffraction patterns of Al-5wt%Pb alloy samples after ball milling for 30 h and then sintering at different temperatures (573, 623, 673 and 723 K) for 1 h. After ball milling for 30 h, only diffraction peaks for Al and Pb are observed; shifts of peak positions have not been detected. No trace of amorphous or other intermediate phases is found. It is also evident that the diffraction peaks of both Al and Pb phases significantly broaden after milling, suggesting that grains of Al and Pb are refined. The broadening of the Pb diffraction peaks is much greater than the broadening of the Al diffraction peaks perhaps because of the softness of the Pb phase. As estimated from the diffraction peak broadening by the Vogit method<sup>[21]</sup>, the average grain sizes of Al and Pb phases are approximately 70 and 7 nm, respectively, demonstrating the formation of the Al-Pb nanocomposite alloy. The diffraction patterns of the as-milled Al-Pb alloys change upon sintering, and the variation is mainly reflected in the extent of peak broadening. This is because only Al and Pb phases exist in all samples and the main microstructure variation is the grain growth in sintering process, as shown in Fig.2, where

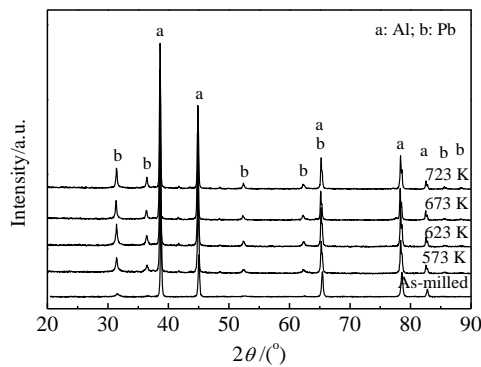


Fig.1 XRD patterns of the as-milled Al-5wt%Pb alloy and the alloys sintered at different temperatures for 1 h

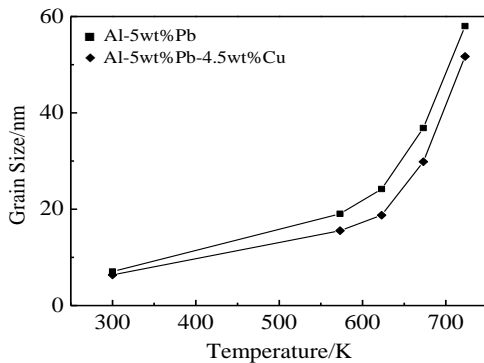


Fig.2 Temperature dependence of the size of Pb phase in MA Al-5wt%Pb and Al-5wt%Pb-4.5wt%Cu alloys (dwelling time: 1 h)

there is an obvious trend that the grain size of Pb phase increases with the increasing of sintering temperature.

Fig.3a shows a TEM bright field image of Al-5wt%Pb sample milled for 30 h. It can be seen that Pb particles with nanometer size embedded in Al matrix are single crystal particles. Therefore, the grain size of Pb phase estimated from XRD analysis represents the size of Pb particles. The average grain size is about 10 nm, which is in good agreement with the XRD result. Fig.4a shows the back scattering electron (BSE) image, in which the dark and bright region represent the Al matrix and Pb particles, respectively, of Al-5wt%Pb sample sintered at 723 K for 1 h after 30 h of milling. The SEM observation shows that the Pb phase grows upon sintering and the Pb particles are homogeneously distributed in Al matrix.

In order to clarify the coarsening kinetics of Pb phase in Al-5wt%Pb nanocomposite alloys, the dependence of Pb phase size on sintering dwelling time was determined, as illustrated in Fig.5. It is clear that there exists an excellent linear correlation between the cubic Pb phase size ( $r$ ) and the dwelling time ( $t$ ) for Al-5wt%Pb nanocomposite alloy at the sintering temperature used. Here,  $r_0$  is the average

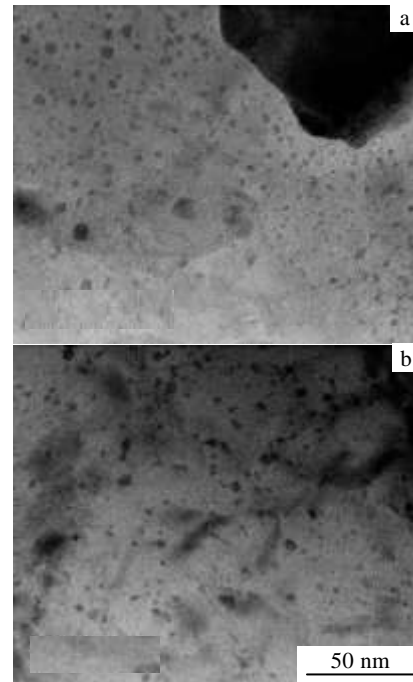


Fig.3 TEM bright field images of as-milled Al-5wt%Pb (a) and Al-5wt%Pb-4.5wt%Cu (b) alloys

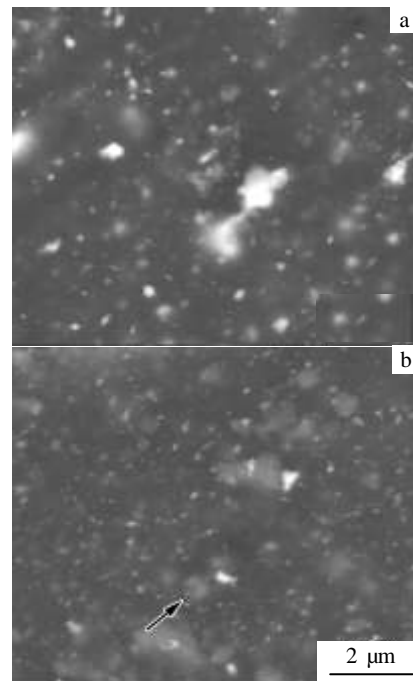


Fig.4 SEM images of as-milled Al-5wt%Pb (a) and Al-5wt%Pb-4.5wt%Cu (b) alloys sintered at 723 K for 1 h (the small bright particles are Pb phase and the arrow indicates the phase rich in Cu)

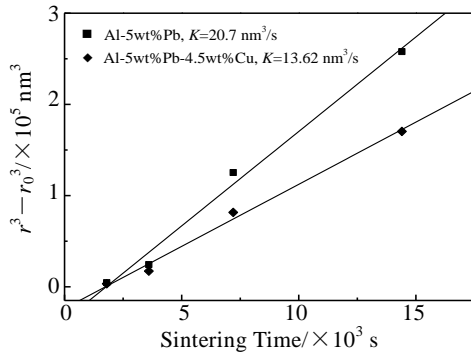


Fig.5 Dependence of the size of Pb phase on sintering time in MA Al-5wt%Pb and Al-5wt%Pb-4.5wt%Cu nanocomposite alloys at sintering temperature of 723 K

radius of the phase in the as-milled condition. It should be indicated that the above linear relationship (in Fig.5) also exists for the Al-5wt%Pb alloy samples sintered at 573, 623 and 673 K. Moreover, it is worth indicating that other power-law dependences, such as  $r^4$  and  $r^6$ , can't yield a satisfactory fitting to the experimental data. The excellent linear relationship between the cubic of  $r$  and  $t$  means that the coarsening of Pb phase in Al-5wt%Pb nanocomposite alloys is controlled by diffusion even though the size of the constituent phase is in the nanometer range.

As mentioned before, the volume fraction of secondary phase did not affect the cubic law of coarsening but would change the value of coarsening rate. Modern Ostwald ripening theories have been developed to account for the effect of volume fraction and predict that the average particle radius ( $r$ ) should increase with time ( $t$ ), according to the equation<sup>[13,14]</sup>:

$$r^3 - r_0^3 = K(\phi)t = \frac{A(\phi)C_e\Omega^2\gamma D}{RT}t \quad (1)$$

where  $\phi$  is the volume fraction of secondary phase, and  $K(\phi)$  is the coarsening rate in modern Ostwald ripening theories, which can be obtained from the slope of the straight line correlated between the cubic  $r$  and time  $t$ , like this in Fig.5.  $A(\phi)$  is a dimensionless constant depending on the volume fraction and  $A(0)=8/9$ ; thus, the theories are simplified to the LSW theory in the limit of zero volume fraction.  $C_e$  is the equilibrium solute content of the matrix,  $\Omega$  is the molar volume of the precipitate,  $\gamma$  is the surface energy per unit area of the matrix-particle phase boundary,  $D$  is the diffusion coefficient of the constitutive particle element in the matrix,  $R$  is the universal gas constant (8.31 J/mol/K) and  $T$  is the coarsening temperature.

By analyzing the coarsening rate  $K(\phi)$ , further details related to coarsening mechanism can be revealed. The interfacial energies ( $\gamma$ ) of solid Pb/Al and liquid Pb/Al calculated by the Miedema model<sup>[22]</sup> are 809.5 and 638 mJ/m<sup>2</sup>,

respectively. The solubility of Pb in Al solid-solution at different temperatures (573, 623, 673 and 723 K) can be calculated according to Ref.[23]. The volume diffusion coefficient  $D$  for solute atoms (Pb) in a solvent matrix (Al) in polycrystalline materials can be obtained from Ref.[24]. However,  $D$  in nanocomposite alloys may be different from that in conventional polycrystalline materials due to the large amount of grain boundaries and phase boundaries which strongly enhance diffusion process. In general,  $D$  has an Arrhenius dependence on temperature:

$$D = D_0 \exp\left(-\frac{Q}{RT}\right) \quad (2)$$

where  $D_0$  is pre-exponential factor and  $Q$  is the coarsening activation energy of secondary phase. The activation energy  $Q$  is often used to characterize the coarsening mechanism. If Eq. (1) is rearranged as

$$\frac{K(\phi)T}{C_e\gamma} = \frac{A(\phi)\Omega^2 D_0}{R} \exp\left(-\frac{Q}{RT}\right) \quad (3)$$

At temperatures from 573 K to 723 K, a linear relationship exists between  $\ln[K(\phi)T/(C_e\gamma)]$  and  $1/T$ , as shown in Fig.6. From its slope, an activation energy of 84.8 kJ/mol for coarsening of Pb phase is obtained for Al-5wt%Pb nanocomposite alloy. This value is much smaller than that of lattice diffusion mechanism of Pb in Al (145.6 kJ/mol<sup>[24]</sup>) and lattice self-diffusion of Al (142.4 kJ/mol<sup>[24]</sup>) but very close to that of boundary self-diffusion of Al (90 kJ/mol<sup>[24]</sup>). This indicates that the coarsening mechanism in the nanocomposite alloys is different from that in conventional grain sized composite alloys. The observation of the cubic law for the coarsening of secondary phase in nanocomposite alloys reveals that the coarsening process is controlled by the three-dimensional long distance diffusion of solute atoms. However, the agreement of the activation energy to that of grain boundary self-diffusion of matrix indicates that the diffusion mechanism in the nanocomposite alloys is basically grain boundary diffusion. This is because the grain sizes of matrix phase and secondary phase are in nanometer range. Thus, the solute atoms should diffuse more easily along nanocrystalline boundary than in conventional grain sized composite alloys.

## 2.2 Effect of Cu addition on the coarsening kinetics of Pb phase in sintering

Fig.7 gives the XRD patterns of Al-5wt%Pb-4.5wt%Cu alloy samples after 40 h milling and then sintered for 1 h at different temperatures (573, 623, 673 and 723 K). Similar to that of Al-5wt%Pb alloy shown in Fig.1, the diffraction peaks of Al and Pb phases broaden apparently in 40 h milled sample, which indicates great refining of their grain size. However, two features different from that of Al-5wt%Pb alloy can be found from the diffraction pattern of the Al-5wt%Pb-4.5wt%Cu alloys. The first is that the diffraction peaks of Al shift to higher angle, indicating the decreasing

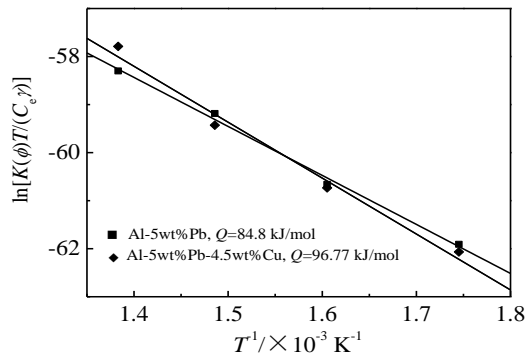


Fig.6 Determination of the activation energy ( $Q$ ) for coarsening of Pb phase in Al-5wt%Pb and Al-5wt%Pb-4.5wt%Cu nanocomposite alloys

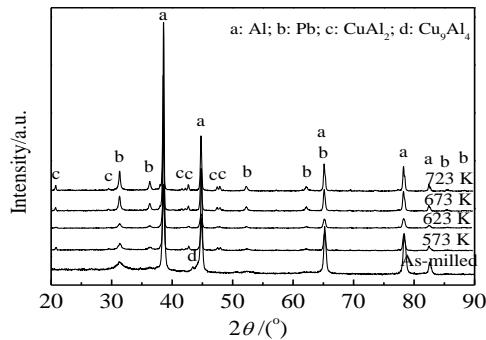


Fig.7 XRD patterns of the as-milled Al-5wt%Pb-4.5wt% Cu alloy and the alloys sintered at different temperatures for 1 h

of lattice constant of Al. The lattice constant of Al is 0.40 448 nm in Al-5wt%Pb-4.5wt%Cu powder milled for 40 h. It means that part of Cu dissolved into Al, forming substitution solid solution. The content of Cu dissolved in Al can be approximately calculated from the lattice constant change according to Vegard's Law. The result shows that the content of Cu dissolved in Al is 1.06 at% after 40 h of milling. The second is that  $\text{CuAl}_2$  and  $\text{Cu}_9\text{Al}_4$  phases are formed after 40 h of milling. However, it is worth noting that the diffraction peaks of Pb phase do not shift apparently, which means that the addition of Cu has not resulted in an obvious alloying effect between Cu and Pb in the present work.

In Fig.7, it can also be seen that the evolution of diffraction patterns depends upon the sintering temperature, which substantially reflects the microstructure change of the as-milled Al-5wt%Pb-4.5wt%Cu alloy in sintering process. At the sintering temperature of 573 K and above, the diffraction peak of  $\text{Cu}_9\text{Al}_4$  phase disappears, while the diffraction peak intensity of  $\text{CuAl}_2$  phase increases. It implies that  $\text{Cu}_9\text{Al}_4$  phase transforms to  $\text{CuAl}_2$  phase in the sintering process. Furthermore, X-ray diffraction measurement proves that the lattice constant of Al is 0.40 465, 0.40 482, 0.40 488 and 0.40 486 nm in the Al-5wt%Pb-4.5wt%Cu sample heated

at 573, 623, 673 and 723 K, respectively for 1 h after MA. In other words, the lattice constant increases towards the value of pure Al. This result means that part of Cu dissolves in Al matrix precipitates and forms  $\text{CuAl}_2$  phase. For Al-5wt%Pb-4.5wt%Cu alloys, the temperature dependence of Pb phase size is also shown in Fig.2, with a comparison to Al-5wt%Pb alloys. It is clear that the grain size of Pb phase in Al-5wt%Pb-4.5wt%Cu alloys increases monotonically with temperature, and is obviously smaller than that in Al-5wt%Pb alloys. This provides concrete evidence of the inhibition of the coarsening of Pb phase by adding Cu constituent in Al-Pb based alloys.

Fig.3b shows a TEM bright field image of Al-5wt%Pb-4.5wt%Cu sample milled for 40 h. It can also be seen that Pb particles with irregular shape and nanometer size are distributed in the Al matrix. The particles of Pb phase is also homogeneously distributed in the Al matrix of as-sintered Al-Pb-Cu samples. Fig.4b shows SEM image of the Al-5wt%Pb-4.5wt%Cu sample sintered at 723 K for 1 h after 40 h of milling. It is observed from the contrast of Fig.4b, that there are two kinds of secondary phase. One is bright small particle which is Pb phase as identified by EDX analysis. The other one, as indicated by the arrows, is grey in contrast. The size of this phase is a little bigger than that of Pb but not very homogenous. EDX analysis proves that the phase is rich in Cu and should contain Cu. As shown in Fig.4, the size of Pb phase in Al-5wt%Pb-4.5wt%Cu alloys is a little smaller than that in Al-5wt%Pb alloys. This is in agreement with the XRD analysis described in a previous section.

The dependence of cubic of Pb size on sintering time in Al-5wt%Pb-4.5wt%Cu alloy sintered at 723 K is also shown in Fig.5. The coarsening rate of Pb phase in Al-5wt%Pb-4.5wt%Cu alloy is also in excellent agreement with the cubic power law, which means that the coarsening of Pb phase is also controlled by diffusion. However, it is apparent that the  $K(\phi)$  value for Al-5wt%Pb-4.5wt%Cu alloy is much smaller than that for Al-5wt%Pb alloy, which means a lower coarsening rate of Pb phase in Al-5wt%Pb-4.5wt%Cu alloy than that in Al-5wt%Pb alloy at the same sintering condition. This is in agreement with the XRD and SEM analysis described before. In other words, the coarsening of Pb phase has been obviously restrained by the addition of Cu in Al-Pb based nanocomposite alloys.

According to Eq.(1), it is apparent that the factors resulting in the difference between the  $K(\phi)$  values in Al-Pb and Al-Pb-Cu alloys are  $A(\phi)$ ,  $D$  and  $\gamma$ . The magnitude of the dimensionless constant  $A(\phi)$  is a monotonically increasing function of the volume fraction of secondary phase. The volume fraction of Pb phase in Al-Pb and Al-Pb-Cu alloys are 0.68% and 0.7%, respectively. The  $A(\phi)$  is less affected by the addition of Cu because of the volume fraction of Pb phase in Al-Pb and Al-Pb-Cu alloys being approximate

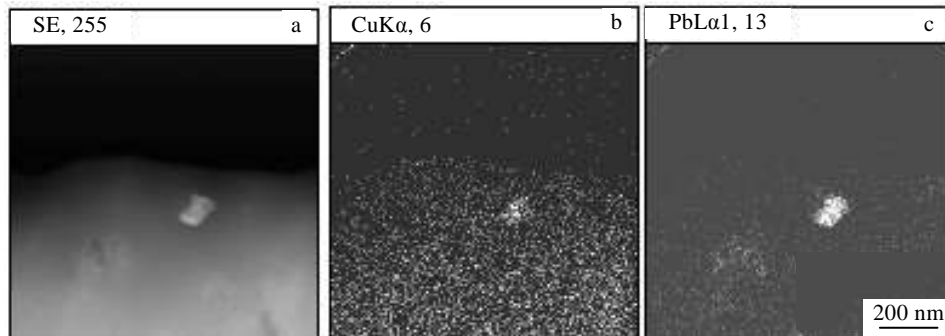


Fig.8 STEM image of a Pb particle inside matrix (a) and element mapping of Cu (b) and Pb (c) in Al-5wt%-4.5wt%Cu alloy sintered at 723 K for 1 h from the powders milled for 40 h

equality. With respect to Al-Pb and Al-Pb-Cu systems, it is likely that  $D$  is also less affected by the addition of Cu because the heat of mixing of Cu-Pb is positive ( $\Delta H=18$  kJ/mol). Thus, the chemical affinity between Cu and Pb is not strong and the drag effect of Cu on Pb is also not strong. However, if Cu segregates at the interface between Al and Pb, the interfacial energy will decrease. Thus, the driven force for coarsening decreases and the coarsening rate of Pb phase in Al-Pb nanocomposite alloys is depressed by the addition of Cu. The interfacial energies of solid Pb/Cu and liquid Pb/Cu calculated by the Miedema model<sup>[22]</sup> are 489 and 249 mJ/m<sup>2</sup>, respectively, which are smaller than that of Al/Pb. Therefore Cu may reduce the interfacial energy between Al and Pb phases. In the present case, as it was found by STEM observation that Cu concentration is high in the area of Pb phase. Fig.8a is a STEM image showing a Pb particle. Fig.8b and 8c show element distribution of Cu and Pb. It is clear that Cu is rich in the Pb area. Using the same method as described before, the coarsening activation energy of Pb phase in Al-5wt%Pb-4.5wt%Cu nanocomposite alloy is obtained, as also shown in Fig.6. It is noted that the Cu addition increases the activation energy  $Q$  for the coarsening of Pb phase.

### 3 Conclusions

1) When annealing at 573, 623, 673 and 723 K for different time, the relation of average particle size of Pb phase in Al-Pb nanocomposite alloys to time obeys the cube law even though the size of the constituent phase is in the nanometer range.

2) The coarsening of Pb phase in Al-Pb nanocomposite alloys is controlled by grain boundary diffusion.

3) Adding Cu decreases the coarsening rate of Pb phase and increases the coarsening activation energy of Pb phase.

### References

- Ma E. *Progress in Materials Science*[J], 2005, 50(4): 413
- Shen T D, Koch C C. *Acta Mater*[J], 1996, 44(2): 753
- Gaffet E, Louison C, Harmelin M et al. *Materials Science and Engineering A*[J], 1991, 134: 1380
- Sheng H W, Zhou F, Hu Z Q et al. *Journal of Materials Research*[J], 1998, 13(2): 308
- Betancourt J I, Davies H A. *Journal of Magnetism and Magnetic Materials*[J], 2002, 246(1-2): 6
- Zhu M, Wang H, Ouyang L Z et al. *International Journal of Hydrogen Energy*[J], 2006, 31(2): 251
- Cha S I, Hong S H, Ha G B et al. *Scripta Mater*[J], 2001, 44(8-9): 1535
- Zhu M, Gao Y, Chuang C Y et al. *Wear*[J], 2000, 242(1-2): 47
- Mahon S W, Song X, Howson M A et al. *Materials Science Forum*[J], 1996, 225-227: 157
- Liu X, Zeng M Q, Ma Y et al. *Wear*[J], 2012, 294-295: 387
- Lifshitz I M, Slyozov V V. *Journal of Physics and Chemistry of Solids*[J], 1961, 19(1-2): 35
- Wagner C. *Berichte Der Bunsengesellschaft Für Physikalische Chemie*[J], 1961, 65: 581
- Baldan A. *Journal of Materials Science*[J], 2002, 37(11): 2171
- Baldan A. *Journal of Materials Science*[J], 2002, 37(12): 2379
- Monzen R, Tada T, Seo T et al. *Materials Letters*[J], 2004, 58(14): 2007
- Johnson W C, Voorhees P W, Zupon D Z. *Metallurgical and Materials Transactions A*[J], 1989, 20(7): 1175
- Del Castillo P E J R D, Reischig P, Van der Zwaag S. *Scripta Materialia*[J], 2005, 52(8): 705
- Yu J H, Kim T H, Lee J S. *NanoStructured Materials*[J], 1997, 9(1-8): 229
- Zhu M, Wu Z F, Zeng M Q et al. *Journal of Materials Science*[J], 2008, 43(9): 3259
- Zhu M, Zeng M Q, Gao Y et al. *Wear*[J], 2002, 253(7-8): 832
- Langford J L. *Journal of Applied Crystalline*[J], 1978, 11(1): 10
- Miedema A R, Den Broeder F J A. *Zeitschrift Für Metallkunde*[J], 1979, 70(1): 14

- 23 Ma E, He J H, Schilling P J. *Physical Review B*[J], 1997, 55(9): 5542
- 24 Gale W E, Totemeier T C. *Smithells Materials Reference Book*[M]. Amsterdam: Butterworth-Heinemann, 2004: 13

## 机械合金化制备具有纳米相复合结构的 Al-Pb 互不溶体系中 Pb 相的粗化动力学和添加 Cu 对其粗化的影响

吴志方, 刘 超, 吴 润, 常庆明

(武汉科技大学 省部共建耐火材料与冶金国家重点实验室, 湖北 武汉 430081)

**摘 要:** 利用 X 射线衍射仪、扫描电子显微镜和透射电子显微镜研究了机械合金化制备的具有纳米相复合结构的 Al-Pb 互不溶体系中 Pb 相的粗化动力学和添加 Cu 对其粗化的影响。结果表明在 573、623、673 和 723 K 退火不同时间后, 尽管 Al-Pb 纳米相复合结构合金中组成相的尺寸均在纳米量级, Pb 相的平均颗粒尺寸与退火时间之间仍满足三次方定律。Pb 相的粗化激活能为 84.8 kJ/mol, 此值接近于基体 Al 的晶界自扩散激活能。这表明 Pb 相的粗化受晶界扩散控制。添加 Cu 降低了 Pb 相的粗化速率, 这与 Cu 在 Al 和 Pb 相的界面偏聚, 降低了 Al/Pb 的界面能有关。添加 Cu 后, Pb 相的长大激活能增加。

**关键词:** 机械合金化; 铝合金; 粗化; 纳米相复合结构合金

---

作者简介: 吴志方, 女, 1977 年生, 博士, 副教授, 武汉科技大学省部共建耐火材料与冶金国家重点实验室, 湖北 武汉 430081, E-mail: wuzhifang@wust.edu.cn